IMPACT DAMAGE MITIGATION USING BIOINSPIRED CFRP LAMINATE ARCHITECTURES

L. Amorim[1], A. Santos[1], M. Branco[2], V. Infante[2], J. P. Nunes[1] and J. C. Viana[1]

[1] IPC/i3N, University of Minho, Guimarães, Portugal
Email: luis.amorim@dep.uminho.pt, Web Page: http://www.ipc.uminho.pt
[2] LAETA, IDMEC, Instituto Superior Técnico, Av. Rovisco Pais, 1049-001 Lisboa, Portugal

Keywords: CFRP, Advanced composites, Bioinspired composites, Low velocity impact, Damage

Abstract

Carbon fibre reinforced polymers (CFRP) are widely used in advanced applications due to their high performance and low weight. However, when exposed to some conditions, as shear, dynamic and impact loading, they may develop interlaminar damages. One of the most common and dangerous solicitations that they must face in service is low velocity impact (LVI) events. To improve damage tolerance to LVI events, three new bioinspired CFRP laminates were developed and tested in the present work to assess and compare their behaviour to the one presented by a typical aeronautic standard laminate. All these studied laminates, having approximately the same thickness of 4 mm, were produced by vacuum bag infusion and observed under reflexion and scanning electron microscopes (SEM) for assessing their processing quality. Interlaminar shear strength (ILSS) and LVI tests were performed in order to evaluate their delamination resistance and impact response. LVI tests were performed for all laminates at the three different impact energy levels of 13.5 J, 25 J and 40 J. Those tests have shown that the bioinspired hybrid laminate (HYB) and all bioinspired ones presented higher interlaminar shear strength and energy absorption for the 40 J impact energy than the standard CFRP laminate (LS), respectively.

1. Introduction

In the last decades, composite materials have been widely used in markets requiring superior performances, such as, the aeronautic, aerospace, military and sports ones [1, 2]. The remarkable mechanical performances and low weight of polymeric composite materials make them more competitive and attractive for high performance applications than the most common traditional materials [3]. Even though advanced composite materials exhibit extraordinary mechanical properties, as stiffness and strength, when submitted to impact, dynamic, flexural conditions, they tend to create fissures inside the laminate, both intralaminar (inside layers) and/or interlaminar (between layers). Such damages are usually related to two major factors: poorer fibre/matrix interface quality and/or lower toughness between the laminate layers [1], [4]–[6]. To overcome these problems, many strategies have been already studied, such as, macro-mechanic though-thickness reinforcements (e.g. 3D-wovens, Z-pinning and stitching), matrix and/or reinforcement modifications and interlaminar toughening [7]–[10].

The insufficient resistance of advanced composite materials to low velocity impact in service is currently one of the major challenges and concerns regarding their application in the mostly demanding markets. The phenomenon can lead to the development of significant damages inside laminate polymeric composites. Due to their inherent brittleness and layer-by-layer nature, a set of complex dissipation energy mechanisms may occur during the impact event leading to the development of delaminations in the laminate without any external visible sign, phenomenon usually called Barely Visible Impact Damage (BVID) [11]. As such damages are problematic and can compromise the performance of any

composite part in service, several works are being carried out in order to understand the mechanisms behind the damage resistance (e.g. damage caused be impact events) and tolerance (composite performance after impact damaged) of these materials [12]. Those studies revealed that thickness, material properties and laminate stack configuration, can play an important role on laminate damage [13]. In fact, it was proven that laminate stack configuration influences the shape and areal damage and, also, dissipation and delamination initiation energy [14, 15]. Recently, a close insight on biological structures, as lobster exoskeletons has shown that their remarkable impact response is attributable to their micro-scale fibrous stacking twisted plywood arrangement [16]–[18]. Inspired on those structures, several authors mimicked them to evaluate their suitability for impact resistance of laminate composites. The results shown that small rotation angle between plies could reduce through-thickness damage after impact, enhance absorbed energy, reduce damaged area and increase penetration resistance [19]–[21]. In this work three new bioinspired composite laminates were produced by vacuum bag infusion and their response to low velocity impact was compared to the one presented by a standard aeronautic CFRP laminate. Interlaminar shear strength tests were also performed and their failure mode was investigated.

2. Composite laminates

2.1. Materials and processing

In this work, CFRP laminates were produced using four different layer architectures, namely: an aeronautic standard (LS), a helical (HL), a helical-symmetric (HL_S) and a hybrid (HYB) laminate. The LS, HL and HL_S laminates were produced using a 150 g/m^2 unidirectional carbon fibre fabric (Dynanotex HS 24/150 DLN2), which corresponds to a thickness of approx. 0.145 mm per final composite layer, whereas much thinner 50 g/m^2 unidirectional fabrics (Dynanotex HS 15/50 SLN2), corresponding to a thickness of approx.. 0.05 mm per layer, were also used to interleave the main laminate layers in the HYB laminate. Both fabrics were provided by G. ANGELONI s.r.l., Italy. As matrix, a bi-component epoxy resin from Sika$^®$ (Biresin$^®$ CR83 epoxy resin and Biresin$^®$ CH83-6 hardener) was selected. The fabrics were first cut considering the different ply angles by using a laser and, then, manually stacked layer-by-layer. All laminates were manufactured by vacuum bag infusion at room temperature and after post-cured inside an oven at 70 ºC during 8 hours. The final composite laminated plates had the dimensions of 350x475 mm and an approximate thickness of 4 mm. Table 1 and Figure 1 show the stack sequences used in the different produced laminates. LS laminate is a standard aeronautic laminate, while HL and HL_S laminates present a bioinspired helical architecture with a pitch angle of 13.3º between plies. Finally, the HYB laminate is a hybrid laminate between LS and bioinspired ones. Its architecture is composed by a symmetrical laminate having 14 main plies reinforced with 150 g/m^2 unidirectional carbon fibre fabrics, being each layer interface interleaved with 3 thinner unidirectional layers (50 g/m^2 unidirectional carbon fibre fabrics) to smooth the angle transition between plies. It should be noted that because some physical twist was always obtained after cure in the final LS laminate due to its unsymmetrical layer stacking sequence, other 28 plies symmetrical laminate with the same pitch angle of 13.3º was also produced (HL_S) to overcome this problem.

Table 1. Laminates stacking sequence.

Laminate Type	Nº of layers 150 g/m^2	*50 g/m^2	Stacking Sequence
LS	28	0	[0/45/90/-45/45/-45/0]$_{2S}$
HL	28	0	[0/13.3/26.6/…/360]
HL_S	28	0	[0/13.3/26.6/…/173.3]$_S$
HYB	14	42	[0/11.25*/22.5*/33.75*/45/55.25*/66.5*/77.75*/90/-77.75*/-66.5*/-55.25*/-45/ -22.5*/0*/22.5*/45/22.5*/0/-22.5*/-45/-33.75*/22.5*/11.25*/0/30*/60*/90*]$_S$

* layers using 50 g/m2 the interleave unidirectional carbon fibre fabric.

L. Amorim, A. Santos, M. Branco, V. Infante, J. P. Nunes and J. C. Viana

2.2. Experimental

2.2.1. Process effectiveness

In order to evaluate the process effectiveness, three samples of each laminate were inspected under the reflexion and scanning electron microscopes (SEM). All the samples were first cut from each laminate plate and then polished to obtain a smooth surface. After preparation, the reflexion microscope from the Institute of Polymers and Composite, at University of Minho was used to evaluate the fibre orientation and presence of voids present in laminates. SEM was also used to deeply evaluate the matrix/fibres adhesion and, also, a closer voids insight.

2.2.2. Interlaminar shear strength (ILSS) tests

Interlaminar shear strength tests were performed in accordance with ISO 14130 standard. The results allow to evaluate and compare how the different laminates architectures influence the interlaminar shear strength, interfacial adhesion and their failure mode. All experiments were performed using a 50 kN Shimadzu universal testing machine at a loading speed of 1 mm/min. Specimens with dimensions of 40 ×20 (mm), which means having a length and a width, respectively, 10 and 5 times higher than its thickness (4 mm), were used in the tests according standard recommendations.
For each specimen, the apparent interlaminar shear strength, τ, was calculated from the obtained data, as:

$$\tau = \frac{3}{4} \times \frac{F}{bh} \tag{1}$$

where, F, is the maximum load and, b, and, h, are the specimen width and thickness, respectively.

2.2.3. Low velocity impact tests

Low velocity impact tests were performed by using a "Fractovis Plus" drop weight impact testing machine, by Ceast. A 20 mm radio piezoelectric hemispherical steel striker and a total drop mass of 5.045 kg were used throughout the testing campaign. The required impact energy was selected by adjusted the height between the drop tip and the specimen upper surface. For every test, the specimens were held by the means of four clamps with rubber tips to a support steel plate. In the middle of this support steel plate exists a 125x75 mm cavity, below the specimen position to expose it to the impact. Specimens had dimensions of 150 × 100 mm, in accordance with ASTM D7136/D7136M standard. Two specimens from each laminate were submitted to three different impact energies, 13.5 J, 25 J and 40 J. During each impact test the load and time were recorded and the impactor velocity at moment of impact calculated by using the kinetic energy (KE) equation:

$$KE = \frac{1}{2} \times m{v_i}^2 \tag{2}$$

where m is the total drop mass and v_i is the initial impactor velocity.

Furthermore, velocity of the impactor was calculated at any time t by using the numerical integration of the force versus time:

$$v(t) = v_i + gt - \int_o^t \frac{F(t)}{m} dt \tag{3}$$

where $v(t)$ is the impactor velocity at time t, g is the gravitational acceleration and $F(t)$ is the measured load at time t. Finally, the energy absorbed by the specimen at each instant, $E_a(t)$ was calculated, as:

$$E_a(t) = E_{a\,i-1} + \frac{m(v_i^2 - v(t)^2)}{2} \tag{4}$$

L. Amorim, A. Santos, M. Branco, V. Infante, J. P. Nunes and J. C. Viana

3.   Results and discussion

The thicknesses were measured and the fibre volume fraction was obtained by calcination (5 samples in furnace at 600ºC during 10 min) in all laminates before testing. In parallel, the used unidirectional carbon fibres were also calcined, in the same conditions, to determine their loss weight under temperature and allow making necessary corrections to the results obtained from the tested laminates. Table 2 presents experimental results obtained after making these last described corrections.

Table 2. Laminates properties.

Laminate Type	Thickness (mm)		Fibre volume fraction (%)
	Average	Stand. Dev.	Average
LS	3.86	0.060	58.60
HL	3.83	0.081	60.71
HL_S	3.89	0.094	60.39
HYB	4.36	0.116	52.10

As can be seen from Table 1, the LS, HL and HL_S laminates present almost the same thickness and fibre volume fraction, around 3.9 mm and 60 %, respectively. Despite being thicker (~13 %), HYB laminate shown lower fibre volume fraction (~13 %), when compared to the others laminates.

Reflection microscopy was used to verify fibre orientation on the laminate layers. Figure 1 shows the cross-section observed in each laminate under reflection microscopy (left) in parallel to its respective three-dimensional scheme representation (right).
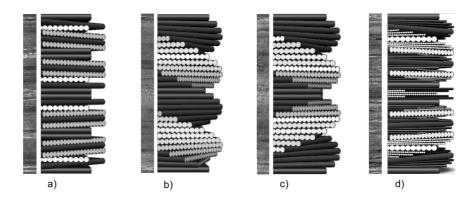

a)   b)   c)   d)

Figure 1. Stack sequence of a) LS, b) HL, c) HL_S and d) HYB laminates under reflection microscopy observation.

SEM observation made also possible to evaluate the effectiveness of resin/fibres adhesion. Figure 2 (left) shows that a good fibre/matrix adhesion was typically observed in all laminates. However, a non-significant number of voids spots were also observed on HL laminate (Figure 2 right).
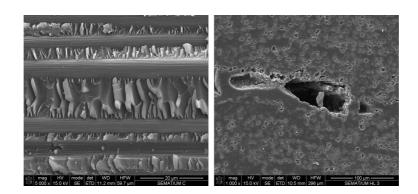
L. Amorim, A. Santos, M. Branco, V. Infante, J. P. Nunes and J. C. Viana

Figure 2. LS laminate SEM visualization of resin/fibres adhesion (5000 x) (left) and void spot observe on HL laminate (1000 x) (right).

The voids observed on bioinspired laminates were somehow expected due to the difficulties found during the vacuum bag processing. Due to the small rotation angles between plies, fibres tend to fill the gaps between each other, turning difficult the resin flow throughout laminate.

Figure 3 shows the apparent interlaminar shear strength results obtained in the ILSS tests. As may be seen, the HYB laminate presented higher interlaminar shear strength than all other laminates (21.9 % higher than LS laminate), whereas HL and HL_S laminates have shown slight lower interlaminar resistance than the LS laminate, 2.8 % and 11.2 % respectively. It was also verified that LS laminate failed in interlaminar shear fracture mode, while the others showed mix mode failure, presenting simultaneously interlaminar shear and though-thickness fracture modes. This seems to be due to the small pitch angle between fibre plies, turning easiest to the crack skip to the next interlaminar interface.
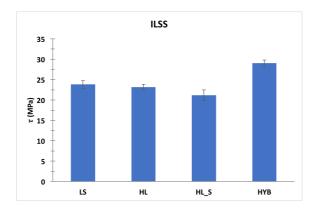

Figure 3. Apparent interlaminar shear strength results.

Two specimens of each laminate were submitted to impact at three different energy levels 13.5 J, 25 J and 40 J. Figure 4 (left) shows the load vs. time history obtained for one specimen of each laminate at 40 J impact energy level. As can be seen, in this case, first the load increases and suddenly drops when a critical load (P_{cr}) is reached. This load represents the instant the first severe damage or delamination occurred in the laminate [22, 23] and, then P_{cr} may be consider as an important damage indicator. As it may be seen at left in Fig. 4, for all developed bioinspired laminates P_{cr} corresponded also to the maximum obtained load, while this didn't happen in LS laminate. Furthermore, this critical occurred later in new bioinspired composites than in the LS one. This indicates that damage occurs first and at lower load and energy in LS composite than in new developed ones.

L. Amorim, A. Santos, M. Branco, V. Infante, J. P. Nunes and J. C. Viana

Figure 4 (right) presents the absorbed energy vs. time obtained from a specimen of each laminate submitted to 40 J impact energy. The final energy plateau on the chart indicates the final amount of dissipated energy that usually is called absorbed energy.
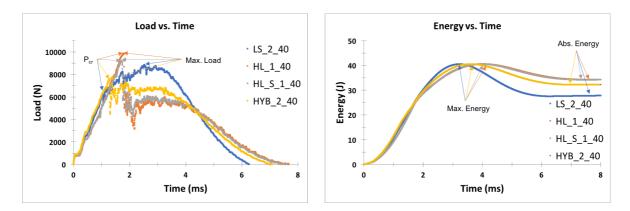

Figure 4. Typical Load vs. Time (left) and Energy vs. Time (right) charts of a specimen of each laminate submitted to 40 J energy impact test.

Figure 5 (left) shows the average of energy absorbed by the specimens for three different impact energies. As it may be seen, for an impact energy of 13.5 J all laminates absorbed circa of 7 J, while when the level of impact energy was increased to 40 J all the new bioinspired composites absorbed approx. 34 J. This shows that these laminates were able to dissipate more energy than the LS one, that only absorbed 28 J. For the 25 J impact energy, the HYB and LS laminates presented similar absorbed energy values (~16 J) while the HL and HL_S ones dissipated slight lower energy levels, 12 J and 14 J, respectively. It is important to note that HYB laminate was slight thicker than the others and this may have some influence the amount of dissipated energy.
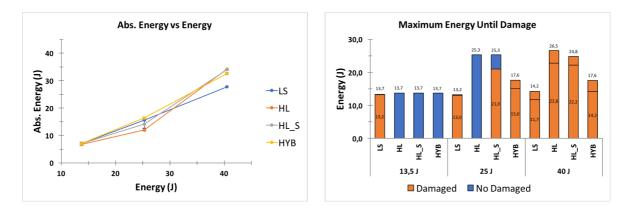

Figure 5. Absorbed Energy vs. Impact Energy (left) and Maximum Energy Until Damage (right).

Not every specimen presented a P_{cr} on load vs. time chart, so it was assumed that in those cases the specimen could receive all the given energy without developing severe damage or delamination. Figure 5 (right) plots, in orange colour, the energy absorbed for each specimen until P_{cr} is reached and, in the cases not presenting P_{cr}, the maximum impact energy at which they have been submitted in blue. All 24 tested specimens (2 from each laminate) submitted to the 13.5 J, 25 J and 40 J energies are plotted on the chart. For the energy of 13.5 J, only one LS specimen presented severe damages, while all the others didn't present any damage. At 25 J, all the specimens of LS and HYB laminates presented

L. Amorim, A. Santos, M. Branco, V. Infante, J. P. Nunes and J. C. Viana

damage, while none of HL specimens and only one of HL_S didn't seem to be severely damaged. When submitted to 40 J impact energy, every specimen exhibited visible damages. Analysing all laminates exposed to the three different energies, LS presented a damage threshold around ~13 J, while for HYB this threshold was slightly higher, ~16 J. Bioinspired laminates revealed to be more resistant until first damage, showing an energy damage threshold close to 25 J.

4. Conclusions

In this work three new bioinspired laminates were compared to a standard aeronautic laminate, all produced by vacuum bag infusion, regarding their interlaminar shear strength and response to low velocity impact. Process effectiveness was confirmed by reflexion and scanning electron microscopy, which had shown a low void amount inside the laminates and a good adhesion between fibres and epoxy resin. The results obtained from ILSS tests showed an increase of 21.9 % in interlaminar shear strength by the HYB laminate, when compared to the others. LVI tests showed an increase on absorbed energy for all new bioinspired laminates than LS one, when submitted to 40 J of impact energy. Concerning the initial damage energy, LS laminates presented a threshold approximately at 13 J while HYB laminates showed a slight increase (~17.6 J). Both bioinspired laminates (HL and HL_S) seems to reach their initial damage energy thresholds close to 26 J. Future work will regard no-destructive evaluation of impacted specimens in order to localize any possible delamination and understand damage mechanisms.

Acknowledgments

References

[1]   M. F. S. F. Moura, A. B. Morais, and A. G. Magalhães, *Materiais Compósitos - Materiais, Fabrico e Comportamento Mecânico*, 1 [a]. Porto: Publindústria, 2005.

[2]   F. A. Administration, "Aviation Maintenance Technician Handbook - Airframe," *Aviat. Maint. Tech. Handb. - Airframe*, vol. 1, p. 588, 2012.

[3]   G. Gardiner, "Aerocomposites: The move to multifunctionality : CompositesWorld," 2015. [Online]. Available: http://www.compositesworld.com/articles/aerocomposites-the-move-to-multifunctionality. [Accessed: 14-Jul-2017].

[4]   K. Kong, O. Kwon, and H. W. Park, "Enhanced mechanical and thermal properties of hybrid SnO2-woven carbon fiber composites using the facile controlled growth method," *Compos. Sci. Technol.*, vol. 133, pp. 60–69, 2016.

[5]   B. X. Yang, K. P. Pramoda, G. Q. Xu, and S. H. Goh, "Mechanical reinforcement of polyethylene using polyethylene-grafted multiwalled carbon nanotubes," *Adv. Funct. Mater.*, vol. 17, no. 13, pp. 2062–2069, 2007.

[6]   F. Gnädinger, P. Middendorf, and B. Fox, "Interfacial shear strength studies of experimental carbon fibres, novel thermosetting polyurethane and epoxy matrices and bespoke sizing agents," *Compos. Sci. Technol.*, vol. 133, pp. 104–110, 2016.

[7]   Y. J. Ma, J. L. Wang, and X. P. Cai, "The effect of electrolyte on surface composite and microstructure of carbon fiber by electrochemical treatment," *Int. J. Electrochem. Sci.*, vol. 8, no. 2, pp. 2806–2815, 2013.

[8]   R. Mezzenga, L. Boogh, and J. A. E. Månson, "A review of dendritic hyperbranched polymer as modifiers in epoxy composites," *Compos. Sci. Technol.*, vol. 61, no. 5, pp. 787–795, 2001.

[9]   A. P. Mouritz, K. H. Leong, and I. Herszberg, "A review of the effect of stitching on the in-plane mechanical properties of fibre-reinforced polymer composites," *Compos. Part A Appl. Sci. Manuf.*, vol. 28, no. 12, pp. 979–991, 1997.

[10]   M. Kuwata, "Mechanisms of interlaminar fracture toughness using non-woven veils as interleaf materials," Queen Mary, University of London, 2010.

[11]   V. Tita, J. de Carvalho, and D. Vandepitte, "Failure analysis of low velocity impact on thin composite laminates: Experimental and numerical approaches," *Compos. Struct.*, vol. 83, no. 4, pp. 413–428, 2008.

[12]   N. H. Nash, T. M. Young, P. T. McGrail, and W. F. Stanley, "Inclusion of a thermoplastic phase to improve impact and post-impact performances of carbon fibre reinforced thermosetting composites - A review," *Mater. Des.*, vol. 85, pp. 582–597, 2015.

[13]   M. Yasaee, I. P. Bond, R. S. Trask, and E. S. Greenhalgh, "Damage control using discrete thermoplastic film inserts," *Compos. Part A Appl. Sci. Manuf.*, vol. 43, no. 6, pp. 978–989, 2012.

[14]   E. Fuoss, P. V Straznicky, and C. Peon, "Effects of stacking sequence on the impact resistance in composite laminates - Part 1 : parametric study," *Compos. Struct.*, vol. 8223, no. 98, 1998.

[15]   C. S. Lopes, O. Seresta, Y. Coquet, Z. Gürdal, P. P. Camanho, and B. Thuis, "Low-velocity impact damage on dispersed stacking sequence laminates . Part I : Experiments," *Compos. Sci. Technol.*, vol. 69, no. 7–8, pp. 926–936, 2009.

[16]   C. A. Melnick, Z. Chen, and J. J. J. Mecholsky, "Hardness and toughness of exoskeleton material in the stone crab, *Menippe mercenaria*," *J. Mater. Res.*, vol. 11, no. 11, pp. 2903–2907, 1996.

[17]   P. Y. Chen, A. Y. M. Lin, J. McKittrick, and M. A. Meyers, "Structure and mechanical properties of crab exoskeletons," *Acta Biomater.*, vol. 4, pp. 587–596, 2008.

[18]   H. O. Fabritius, C. Sachs, P. R. Triguero, and D. Raabe, "Influence of structural principles on the mechanics of a biological fiber-based composite material with hierarchical organization: The exoskeleton of the lobster homarus americanus," *Adv. Mater.*, vol. 21, no. 4, pp. 391–400, 2009.

[19]   T. Apichattrabrut and K. Ravi-Chandar, "Helicoidal Composites," *Mech. Adv. Mater. Struct.*, vol. 13, no. 1, pp. 61–76, 2006.

[20]   L. K. Grunenfelder *et al.*, "Bio-inspired impact-resistant composites," *Acta Biomater.*, vol. 10, no. 9, pp. 3997–4008, 2014.

[21]   D. Ginzburg, F. Pinto, O. Iervolino, and M. Meo, "Damage tolerance of bio-inspired helicoidal composites under low velocity impact," *Compos. Struct.*, vol. 161, pp. 187–203, 2017.

[22]   D. D. R. Cartié and P. E. Irving, "Effect of resin and fibre properties on impact and compression after impact performance of CFRP," *Compos. - Part A Appl. Sci. Manuf.*, vol. 33, no. 4, pp. 483–493, 2002.

[23]   X. Zhang, L. Hounslow, and M. Grassi, "Improvement of low-velocity impact and compression-after-impact performance by z-fibre pinning," *Compos. Sci. Technol.*, vol. 66, no. 15, pp. 2785–2794, 2006.